



## Phenol degradation by powdered metal ion modified titanium dioxide photocatalysts

Khraisheh, M., Wu, L., Al-Muhtaseb, A. H., Albadarin, A. B., & Walker, G. M. (2012). Phenol degradation by powdered metal ion modified titanium dioxide photocatalysts. *Chemical Engineering Journal*, 213(null), 125-134. DOI: 10.1016/j.cej.2012.09.108

**Published in:**  
Chemical Engineering Journal

**Document Version:**  
Peer reviewed version

**Queen's University Belfast - Research Portal:**  
[Link to publication record in Queen's University Belfast Research Portal](#)

**Publisher rights**  
This is the author's version of a work that was accepted for publication in *Chemical Engineering Journal*. Changes resulting from the publishing process, such as peer review, editing, corrections, structural formatting, and other quality control mechanisms may not be reflected in this document. Changes may have been made to this work since it was submitted for publication. A definitive version was subsequently published in *Chemical Engineering Journal*, Vol. 213, 01/12/2012.

**General rights**  
Copyright for the publications made accessible via the Queen's University Belfast Research Portal is retained by the author(s) and / or other copyright owners and it is a condition of accessing these publications that users recognise and abide by the legal requirements associated with these rights.

**Take down policy**  
The Research Portal is Queen's institutional repository that provides access to Queen's research output. Every effort has been made to ensure that content in the Research Portal does not infringe any person's rights, or applicable UK laws. If you discover content in the Research Portal that you believe breaches copyright or violates any law, please contact [openaccess@qub.ac.uk](mailto:openaccess@qub.ac.uk).

## Accepted Manuscript

Phenol degradation by powdered metal ion modified titanium dioxide photocatalysts

Majeda Khraisheh, Lijun Wu, Ala'a H. Al-Muhtaseb, Ahmad B. Albadarin, Gavin M. Walker

PII: S1385-8947(12)01312-5  
DOI: <http://dx.doi.org/10.1016/j.cej.2012.09.108>  
Reference: CEJ 9869

To appear in: *Chemical Engineering Journal*

Received Date: 17 May 2012  
Revised Date: 19 September 2012  
Accepted Date: 21 September 2012

Please cite this article as: M. Khraisheh, L. Wu, A.H. Al-Muhtaseb, A.B. Albadarin, G.M. Walker, Phenol degradation by powdered metal ion modified titanium dioxide photocatalysts, *Chemical Engineering Journal* (2012), doi: <http://dx.doi.org/10.1016/j.cej.2012.09.108>

This is a PDF file of an unedited manuscript that has been accepted for publication. As a service to our customers we are providing this early version of the manuscript. The manuscript will undergo copyediting, typesetting, and review of the resulting proof before it is published in its final form. Please note that during the production process errors may be discovered which could affect the content, and all legal disclaimers that apply to the journal pertain.



1 **Phenol degradation by powdered metal ion modified titanium dioxide photocatalysts**

2  
3  
4 Majeda Khraisheh<sup>a</sup>, Lijun Wu<sup>b</sup>, Ala'a H. Al-Muhtaseb<sup>c</sup>, Ahmad B. Albadarin<sup>d</sup>, Gavin M.  
5 Walker<sup>d,e</sup>

6  
7  
8 <sup>a</sup> Department of Chemical Engineering, College of Engineering, Qatar University, P.O. Box  
9 2713, Qatar

10  
11 <sup>b</sup> Department of Civil, Environmental and Geomatic Engineering  
12 University College London, UK

13  
14  
15 <sup>c</sup> Petroleum and Chemical Engineering Department, Faculty of Engineering, Sultan Qaboos  
16 University, P.O. Box 33, Al-khod 123, Oman

17  
18  
19 <sup>d</sup> The Queen's University Environmental Science and Technology Research Centre, School of  
20 Chemistry and Chemical Engineering, Queen's University Belfast, Northern Ireland, UK.

21  
22 <sup>e</sup> Materials Surface Science Institute, Department of Chemical and Environmental Sciences,  
23 University of Limerick, Ireland

24  
25  
26  
27 \* Corresponding author

28  
29  
30  
31 Gavin M. Walker  
32 E-mail: [g.walker@qub.ac.uk](mailto:g.walker@qub.ac.uk)

46 **Abstract**

47  
48 Conventional water purification and disinfection generally involve potentially hazardous  
49 substances, some of which known to be carcinogenic in nature. Titanium dioxide photocatalytic  
50 processes provide an effective route to destroy hazardous organic contaminants. This present  
51 work explores the possibility of the removal of organic pollutants (phenol) by the application of  
52 TiO<sub>2</sub> based photocatalysts. The production of series of metal ions doped or undoped TiO<sub>2</sub> were  
53 carried out via a sol gel method and a wet impregnation method. Undoped TiO<sub>2</sub> and Cu doped  
54 TiO<sub>2</sub> showed considerable phenol degradation. The efficiency of photocatalytic reaction largely  
55 depends on the photocatalysts and the methods of preparation the photocatalysts. The doping of  
56 Fe, Mn, and humic acid at 1.0 M% via sol gel methods were detrimental for phenol degradation.  
57 The inhibitory effect of initial phenol concentration on initial phenol degradation rate reveals that  
58 photocatalytic decomposition of phenol follows pseudo zero order reaction kinetics. A  
59 concentration of >1 g/L TiO<sub>2</sub> and Cu doped TiO<sub>2</sub> is required for the effective degradation of 50  
60 mg/L of phenol at neutral pH. The rise in OH<sup>-</sup> at a higher pH values provides more hydroxyl  
61 radicals which are beneficial of phenol degradation. However, the competition among phenoxide  
62 ion, Cl<sup>-</sup> and OH<sup>-</sup> for the limited number of reactive sites on TiO<sub>2</sub> will be a negative influence in  
63 the generation of hydroxyl radical. The dependence of phenol degradation rate on the light  
64 intensity was observed, which also implies that direct sunlight can be a substitute for the UV  
65 lamps and that photocatalytic treatment of organic pollutants using this technique shows some  
66 promise.

67  
68 *Keyword:* Photocatalysts; Modified titanium dioxide; Photoreactor; Sol gel method; Wet  
69 impregnation method; Phenol;

## 70 1- Introduction

71 While the world's population tripled in the 20th century, the use of renewable water resources  
72 has grown six-fold. Poor access to good quality drinking water increases the risk of waterborne  
73 diseases, which result in more than 10 million deaths. Diarrhoea alone is responsible for 2.2  
74 million deaths each year, mostly among children under the age of five. This represents a  
75 significant global problem, however a number of options available today for water disinfection  
76 include chlorination, ozonation, iodine treatment, UV treatment, and boiling [1]. The ideal  
77 solution would offer complete and full sterilization, without harming other forms of life; it  
78 should also be inexpensive as well as non-corrosive [2].

79 The last 20 years has seen the development of two of the most interesting disinfection  
80 alternatives: solar disinfection and  $\text{TiO}_2$  photodisinfection under UV illumination [3]. The  
81 combination of the two methods would result in a much greener, cheaper, more efficient, less  
82 energy consuming technology, which could be produced and widely applied whilst causing no  
83 harm to human health. Considering the fact that the areas of the world that lack access to safe  
84 drinking water, which are also the world's poorest nations, have an abundance of sunlight  
85 irradiation, the provision of this new technique can alleviate the current burden on the global  
86 water supply and improve sanitation. However, the band-gap of  $\text{TiO}_2$  is large, and is only active  
87 in the ultraviolet region ( $<400\text{nm}$ ), which is  $< 10\%$  of the overall solar intensity, therefore the  
88 light harvesting ability of  $\text{TiO}_2$  is very limited [4]. The challenges in this area are the  
89 development and mechanism investigation of an efficient  $\text{TiO}_2$  based photocatalyst, which is  
90 workable under sunlight [5]. Among many catalyst improvement techniques, doping has been  
91 shown to be one of the most promising options, however its application in water disinfection  
92 requires further investigation. Current photocatalysis is mainly focused on  $\text{TiO}_2$ , and the basis for

93 its use is the employment of sunlight (or an artificial solar simulator lamp system) as an energy  
94 input so that TiO<sub>2</sub> can be photoactivated by the UV spectrum of the irradiation [6].  
95 The work of Matsunaga et al. [7] showed that TiO<sub>2</sub> was effective in photokilling *Lactobacillus*  
96 *acidophilus* (gram-positive bacteria), *Saccharomyces cerevisiae* (yeast) and *Escherichia coli*  
97 (gram-negative bacteria) under a metal halide lamp (12000  $\mu\text{e}\cdot\text{m}^{-2}\cdot\text{s}^{-1}$ ) for 1-2 h, moreover a  
98 mechanism involved in the photooxidation of CoA was proposed. Ireland et al. [8] found that  
99 the addition of electron acceptor-hydrogen peroxide at millimolar level had a positive impact on  
100 the disinfection capability. Ide et al. [9] reported that the presence of deposited Au on the  
101 supported layered TiO<sub>2</sub> could significantly improve its photocatalytic activity in the visible light  
102 range. Zhang et al. [10] found that the absorption edge of N,S-codoped TiO<sub>2</sub> had a red-shift and  
103 possessed the photocatalytic efficiency under visible light. Li et al. [11] proposed a visible  
104 semiconductor sensitizer BiOI, which exhibits excellent photocatalytic activities on the  
105 degradation of phenol under visible light irradiation. Photocatalytic tests showed that BiOI is an  
106 effective sensitizer for improving the visible light photocatalytic activity of TiO<sub>2</sub>. Zhu et al. [12]  
107 investigated the photocatalytic disinfection of *E. coli* 8099 using Ag/BiOI composites under  
108 visible light irradiation. The experimental results showed that the photocatalytic disinfection  
109 efficiency of *E. coli* ( $5 \times 10^7$  cfu mL<sup>-1</sup>) using 2.09%Ag/BiOI was almost 99.99% within 10 min  
110 irradiation. Photocatalytic silver doped titanium dioxide nanoparticles (nAg/TiO<sub>2</sub>) were  
111 investigated for their capability of inactivating bacteriophage MS2 in aqueous media [13]. The  
112 inactivation rate of MS2 was enhanced by more than 5 fold depending on the base TiO<sub>2</sub> material,  
113 and the inactivation efficiency increased with increasing silver content. The increased production  
114 of hydroxyl free radicals was found to be responsible for the enhanced viral inactivation.

115 Sontakke et al. [14] studied the photocatalytic inactivation of Escherichia coli with combustion  
116 synthesized TiO<sub>2</sub> photocatalysts in the presence of visible light. It was found that photolysis  
117 alone had a small effect on inactivation while the dark experiment resulted in no inactivation and  
118 Ag/TiO<sub>2</sub> showed the maximum inactivation. At a catalyst loading of 0.25 g/L, all the combustion  
119 synthesized catalysts showed better inactivation of E. coli compared to commercial Degussa P-  
120 25 (DP-25) TiO<sub>2</sub> catalyst. An improved inactivation was observed with increasing lamp intensity  
121 and addition of H<sub>2</sub>O<sub>2</sub>. A negative effect on inactivation was observed by addition of inorganic  
122 ions such as HCO<sub>3</sub><sup>-</sup>, SO<sub>4</sub><sup>2-</sup>, Cl<sup>-</sup>, NO<sub>3</sub><sup>-</sup>, Na<sup>+</sup>, K<sup>+</sup>, and Ca<sup>2+</sup>. The photocatalytic inactivation of E.  
123 coli remained unaltered at different pH of the solution.

124  
125 However, problems such as the instability of the metal-doped titania and relatively low  
126 absorption efficiency of the nonmetal-doped titania in the visible light region, are still  
127 unresolved. Thus, exploring the highly-active photocatalysts with narrow band gap, which  
128 function in the visible light region, has attracted remarkable attention. Accordingly, the aim of  
129 this work was to explore the possibility of the removal of an organic pollutant (phenol) by the  
130 application of TiO<sub>2</sub> based photocatalysts. The production of series of metal ions doped or  
131 undoped TiO<sub>2</sub> was undertaken by a sol gel method and a wet impregnation method. A standard  
132 photoreactor system was designed for such a purpose and the transport/kinetic processes of  
133 phenol adsorption and removal were investigated.

134

135

136

137

138

## 139 2- Materials and Methods

### 140 2.1. Preparation of TiO<sub>2</sub> based photocatalysts

#### 141 142 2.1.1 Sol-gel method

143 Materials used in this method are shown in Table (1). All the chemicals were laboratory grade. In  
144 this method, Titanium (IV) isopropoxide was selected as metal alkoxide precursor because a  
145 metal alkoxide with larger molecular weight is relatively stable, which is important in controlling  
146 the reaction rate. Isopropanol, 2 (2-ethoxyethoxy) ethanol and ethanol were used as stabilizing  
147 agents and solvents for the otherwise immiscible TTIP and H<sub>2</sub>O. HCl and H<sub>2</sub>SO<sub>4</sub> were used as  
148 hydrolysis catalysts, while CuCl<sub>2</sub>, CuSO<sub>4</sub> and Cu(NO<sub>3</sub>)<sub>2</sub> were employed as dopants.  
149 Undoped and Cu/TiO<sub>2</sub> catalysts were prepared via a sol gel method described by Ding and Liu  
150 [15]. Titanium (IV) isopropoxide and alcohol (ethanol, 2(2-ethoxyethoxy) ethanol or  
151 isopropanol) were vigorously stirred in a beaker. A mixture of fixed amount of deionised water  
152 (DI water), acid (HCl or H<sub>2</sub>SO<sub>4</sub>) and alcohol was added drop-wise into the previous  
153 TTIP/alcohol solution and magnetically stirred. After gelation, it was dried at 60°C in an oven  
154 overnight. The powder was then annealed at a specific temperature for 2 h in furnace. Finally,  
155 the catalysts was pulverized through 75µm sieves and kept in a sealed jar for use. For Cu doped  
156 TiO<sub>2</sub>, a given amount of copper precursor (1 ~ 10 mol % to TiO<sub>2</sub>) was mixed with DI water, acid  
157 and alcohol solution before the mixture was added into a TTIP/alcohol solution. The rest of the  
158 preparation procedure was the same as with undoped TiO<sub>2</sub>.

#### 160 2.1.2 Wet-impregnation method

161 Materials used in this method are shown in Table (1). The preparation of Cu doped catalysts was  
162 via a wet impregnation method described by Di paola et al. [16]. A given type/amount of Copper  
163 dopant and TiO<sub>2</sub> P25 were added to 100 mL DI water. The mixture was then magnetically stirred



164 24 h followed by washing three times using DI water through filtration. Finally, solid was oven  
165 dried at 60°C. Further calcination was carried out at 500°C for 2 h.

## 166 *2.2 Designation of prepared photocatalysts*

167  
168 The denotation of the final catalysts was based on some of synthesis variables, including  
169 preparation method, undoped or doped, difference in starting solution composition and annealing  
170 temperature. The name of a catalyst can be seen in the format of ATBC. Here “A” stands for the  
171 preparation method, it can be sol-gel method (SG) or Wet-impregnation method (IM). “T” is  
172 short for TiO<sub>2</sub> and means it is a TiO<sub>2</sub> based photocatalyst. “B” stands for a dopant which could  
173 be iron (Fe), Humic acid (HA), Manganese (Mn) but in most cases, it is copper (Cu). “C” stands  
174 for different conditions in starting solution composition and annealing temperature, a detailed  
175 lists corresponding to this nomenclature can be found in the list of synthesised materials. For  
176 example, SGT9 represents a TiO<sub>2</sub> based photocatalyst, which was prepared by the sol-gel  
177 method. In the standard sol gel procedure, the starting solution is composed of TTIP, Ethanol,  
178 HCl and H<sub>2</sub>O at a molar ratio of 1:8:0.06:1. There is no dopant addition in the dried catalysts and  
179 the final annealing is at a temperature of 500°C for 2 h. Similarly, SGTCu43 is a TiO<sub>2</sub> based  
180 photocatalyst which prepared from sol-gel method. In the standard sol-gel procedure, the starting  
181 solution is composed of TTIP, isopropanol, H<sub>2</sub>SO<sub>4</sub> and H<sub>2</sub>O at a molar ratio of 1:80:0.06:14. It  
182 was doped by copper at a level of 0.1 mol% towards TiO<sub>2</sub> and the final annealing conditions are  
183 600°C for 2 h. The system with wet impregnated samples is simpler, they all share a same  
184 starting TiO<sub>2</sub> P25 aqueous mixture and therefore, the number 2 in IMTCu2 stands for dopant  
185 CuCl<sub>2</sub> is introduced at a level of 1.0 mol% before 500°C for 2 h.

186

187

188 *2.3 Measurement of photocatalytic activity*

189

190 *2.3.1 Solar box system*

191

192 The photoreactor consists of two chambers: the lamp and reactor chamber, with the lamp  
193 chamber installed on top of the reactor chamber. Two UVA lamps are located in the lamp  
194 chamber: (i) a commercial rupture fluorescent tube lamp and (ii) a fluorescent Blacklight Blue  
195 tube lamp (18W, Silva) which transmit ultraviolet radiation peaking at 365 nm. In the reactor  
196 chamber, Pyrex glass flasks are employed as batch reactors. Water samples taken from the solar  
197 box system at specific time intervals were run at UV-Vis spectrophotometry for phenol  
198 degradation experiment.

199

200 *2.3.2 Continuous flow system*

201 The schematic experimental set up for continuous flow system is shown in Figure (1). It  
202 essentially consists of a photocatalytic reactor (PCR) with rectangle cooling jacket. Tap water is  
203 circulated in the cooling jacket to control the temperature of PCR at 25°C (if not otherwise  
204 stated). The PCR contains a UV lamp, 1 g/mL photocatalysts and magnetic stirrer. The aqueous  
205 liquid running up the reactor was perpendicularly illuminated by immersed UV lamp whose  
206 irradiation consistently strikes on the photocatalysts suspension. All parts of this reactor are  
207 made from stainless steel in order to enhance the refracted light intensity. Photocatalysts are  
208 located inside the inner circle container. Other main components of the system are the control  
209 valve, the water grab sampler, a filter, connecting tubes and a water reservoir. The main function  
210 of the water tank (WT) is to provide aeration of circulating bacterial suspension. The water grab  
211 sampler is made up of water pump and flow meter, which provide the flow of the liquid in the  
212 system. To sieve the photocatalyst, a filter has been incorporated downstream of the system. The  
213 size of the PCR is around 700 cm<sup>3</sup> and the total volume (V) of water suspension in the system is

214 controlled at  $2000 \text{ cm}^3$  with the flow rate varied from 25 to  $125 \text{ cm}^3 \text{ min}^{-1}$ .

215

#### 216 *2.4 Phenol photodegradation in water*

217

218 The evaluation of decontamination ability of the prepared catalysts was assessed by  
219 photooxidation of phenol in water in the solar box system. To compare the degradation rates  
220 between samples, it was ensured that the initial phenol concentration and irradiation intensity  
221 were as close as possible. The evolution of the phenol concentration was monitored by UV–vis  
222 spectrophotometry at its characteristic 270 nm band, using a centrifuged (4500 r.p.m for 5min)  
223 aliquot ca. 2 mL of the suspension. All experiments were carried out in triplicates and DI water  
224 was used throughout.

#### 225 *2.5 Characterization and analytical tools*

##### 226 *2.5.1 Point of zero charge determination*

227 In the experiment procedure described by Reymond and Kolenda: oxide suspensions with the  
228 catalysts solid contents (weight percentage) as 0.01%,0.1%,1%,5%,10% were introduced in glass  
229 beakers (capacity:10 mL). The beakers were filled with catalysts oxide suspensions in DI water  
230 before sealed in order to minimize the residual air volume above suspension. The beakers were  
231 then kept in air and shaken at 200 rpm at room temperature for 24 h. The pH was measured after  
232 24 h of contact time, time for which pH equilibrium was reached in all the cases. It is considered  
233 that the PZC value of the oxide is the pH value of the suspension having the higher solid content  
234 when pH evolution with solid concentration is low.

### 235 2.5.2 Surface area measurement

236 The sample was pre-treated at 368 K for 1 h and 573K for 3 h under nitrogen, and then a  
237 conventional 5-point BET nitrogen isotherm was taken at 77 K. All measurements were carried  
238 out on a Micromeretics Gemini analyser. The amount of nitrogen admitted to the catalyst sample  
239 was logged and the surface area calculations were carried out by the analyser.

### 240 2.5.3 UV-vis spectrophotometer

241 The concentration of phenol was measured on a double beam spectrophotometer (M350 double  
242 beam, Camspec Scientific Instruments Ltd, Sawston, Cambridge, UK). To avoid the imperfection  
243 of matching cuvettes when using a double beam, only one beam was used with a 1 cm quartz  
244 cuvette. The zero was achieved with DI water and cuvette was regularly left to soak in  
245 concentrated hydrochloric acid. The spectra of absorption of the phenol indicates the existence of  
246 an absorption band corresponding to the transition  $n \rightarrow n^*$  to a wavelength of 270 nm. The  
247 indicated absorbance is proportional to the concentration in phenol, according to the law of Beer  
248 Lambert in the studied concentration domain 0 - 100 mg/l.

249

## 250 3- Results and Discussion

### 251 3.1 Preliminary results

252 Preliminary tests were undertaken to check the viability of the solar box as a light input system.  
253 A series of doped  $\text{TiO}_2$  were prepared using the standard sol gel method as detailed in section  
254 2.1.1 and a brief summary is provided in Table (2). The length of experiment was extended to 24  
255 h in order to set a proper sampling time interval for later experiments. A typical trail time would  
256 be set at around 10 h with 2 h sampling intervals. Blank samples were introduced using  
257 irradiated phenol without the addition of photocatalysts.

258 As shown in Figure (2), the prepared dopant-free TiO<sub>2</sub> photocatalyst was very effective in the  
259 reaction of phenol decomposition, and a linear dependence of phenol concentration versus time  
260 was obtained. An analogous linear dependence was also observed for other doped TiO<sub>2</sub>. From  
261 these, consistent data were obtained using the Cu doped TiO<sub>2</sub>, therefore, this was selected for  
262 further investigations. On the other hand, humic acid doped TiO<sub>2</sub> and Mn doped TiO<sub>2</sub> (1 mol%  
263 dopant: Ti<sup>4+</sup>) are almost photochemically inactive and low photoreactivity for phenol degradation  
264 is observed for Fe<sup>3+</sup> doped TiO<sub>2</sub>.

265 The effect of individual metal ions on the photocatalytic activity of metal ion doped TiO<sub>2</sub> is a  
266 complex area. An interpretation of reactivity order is difficult since it is probably the net result of  
267 a combination of factors such as surface area, crystallinity, crystal size, band-gap energy etc.  
268 Moreover, the addition of metals could be either beneficial or detrimental depending on whether  
269 such metals decrease the rate of electron-hole recombination or act as electron-hole  
270 recombination centers [17].

271 Using phenol as target organic pollutant and catalysts prepared from sol gel method, a significant  
272 photoactivity decrease in metal ion doped TiO<sub>2</sub> compared with dopant free TiO<sub>2</sub> was also  
273 reported in literature [18] with the dopant ions behaving as recombination centres of the  
274 photoproduced charge carriers. The presence of dopant at a concentration level of 1 mol% seems  
275 to be adequate to produce a negative influence by decreasing the density of surface-active  
276 centers. However, it is still too early to conclude that doping is negative for the photodegradation  
277 reactions. Dominant parameters such as character and concentration of the dopant, preparation  
278 method and reaction regimes could be the key to tune up the reactivity of doped TiO<sub>2</sub>.

279 *3.2 The effect of initial phenol concentration*

280 The photodegradation efficiency of phenol is related closely to its initial concentration. Higher  
281 phenol concentrations lead to a decrease in the degree of degradation within the same time  
282 period. The main reactions occur on the surface of the solid photocatalyst and at a high initial  
283 concentration all catalytic sites are occupied. Further increase in the concentration can provide  
284 excess reactant and also limits the adsorption of reaction intermediate on the reactive surface.  
285 This prohibits the penetration of light reaching the surface and consequently less HO• is formed  
286 resulting in a decrease of the observed zero-order rate constant.

287 The effect of the initial concentration of phenol is presented in Figures (3a) and (3b), and Table  
288 (3). An increase in the initial phenol concentration substantially decreases in the degradation  
289 rate. The remarkable inhibitory effect of the initial concentration of phenol on the apparent rate  
290 constant has been reported with the photocatalytic decomposition of phenol following a negative  
291 first order reaction kinetics [19,20]. However, there is no clear understanding of this negative  
292 influence of initial phenol concentration. It has been proposed [21] that the phenoxide ions ArO<sup>-</sup>,  
293 which are generated from the dissociation of phenol, maybe compete with and replace the  
294 adsorbed OH<sup>-</sup> on the limited number of reactive positions on the surface of catalysts. Then the  
295 generation of OH• will be reduced since there are fewer active sites for the generation of OH•  
296 radicals. It is also worth noting that Phenol is always adsorbed on the TiO<sub>2</sub> surface in a  
297 phenoxide ion [22].

298 At a concentration of 20 mg/L, there seems to be sufficient reactant molecules for the reactive  
299 sites, however, a further increase in the concentration may prohibit the penetration of light.  
300 Meanwhile, an excess phenol concentration increases the concentration of reaction intimidates to  
301 be treated, which in turn also compete with the phenol for the reactive sites on the TiO<sub>2</sub> surface.

302 In the photomineralization of organic pollutants sensitized by TiO<sub>2</sub>, it has been traditionally  
 303 reported that the initial rate of disappearance of the pollutant fits a Langmuir–Hinshelwood (L–  
 304 H) kinetic scheme [23]. The Langmuir-Hinshelwood (L-H) kinetic model assumes rapid,  
 305 reversible adsorption of a reactant on the catalyst surface prior to reaction. The L-H rate equation  
 306 is of the form:

$$307 \quad r_o = -\frac{d[C]}{dt} = \frac{k.K[C]}{1 + K[C]} \quad (1)$$

308 Where:  $r_o$  is the initial rate of disappearance of the organic substrate;  $k$  is a rate constant for the  
 309 reaction ( $\text{mmol L}^{-1} \text{min}^{-1}$ ), reflecting the limiting rate of reaction at maximum coverage under the  
 310 given experimental conditions;  $K$  is the constant for adsorption of the organic substrate onto the  
 311 TiO<sub>2</sub> surface ( $\text{L mmol}^{-1}$ ); and  $C$  is the concentration of the organic substrate ( $\text{mmol L}^{-1}$ ) in  
 312 solution.  
 313

314 The above equation can be inverted to solve for  $k$  and  $K$ .

$$315 \quad \frac{1}{r_o} = \frac{1}{K} + \frac{1}{k.K[C]} \quad (2)$$

316  
 317 The slope and intercept from a plot of  $1/r_o$  versus  $1/[C]$  can be used to determine  $k$  and  $K$ .  
 318  
 319 Phenol oxidation data for both undoped and Cu doped TiO<sub>2</sub> at pH 5 were plotted using Equation  
 320 (2) with reasonably good fits ( $R^2 > 0.95$ ). The rate constant and the binding constant for TiO<sub>2</sub>  
 321 catalyst are  $-0.16 \times 10^{-3} \text{ mmol L}^{-1} \text{ min}^{-1}$  and  $-17.57 \text{ L mmol}^{-1}$ , respectively, while for Cu/TiO<sub>2</sub>  
 322 they are  $-0.5 \times 10^{-4} \text{ mmol L}^{-1} \text{ min}^{-1}$  and  $-15.67 \text{ L mmol}^{-1}$ , respectively. Traditionally,  $k$  is taken to  
 323 represent the Langmuir absorption constant of the species (organic substrate) on the surface of  
 324 TiO<sub>2</sub>, and  $K$  is a proportionality constant which provides a measure of the intrinsic reactivity of  
 325 the photoactivated surface with organic substrate [23]. The L-H rate constants at pH = 6.3

326 derived from Equation (2) for both catalysts showed the same order of reactivity, but the  
327 undoped  $\text{TiO}_2$  is almost 3 times more active than Cu doped  $\text{TiO}_2$ . However, it is generally  
328 assumed that both rate constants and orders are only “apparent”. They serve to describe the rate  
329 of degradation, and may be used for reactor optimization, but they have no physical meaning,  
330 and may not be used to identify surface processes.

### 331 *3.3 The effect of catalyst dose*

332 To increase the performance of heterogeneous photocatalytic process, one common way is to  
333 increase the contact area of  $\text{TiO}_2$  along the light path. The amount of catalyst used is also related  
334 to cost effectiveness. A low mass of catalyst requires an extension of light exposure and  
335 hydraulic retention time which increases the cost effectiveness. On the other hand, an excessive  
336 amount of catalyst has cost implications and potential to reduce photoactivity due to increased  
337 turbidity of the suspension. Hence, it is important to find the optimal amount catalyst mass for  
338 the system.

339 To study the influence of catalyst mass, the quantity of catalyst was varied whilst keeping the  
340 concentration of phenol solution equal to 50 mg/L. Figures (4a) and (4b) illustrated the influence  
341 of catalyst mass on the degradation of phenol, in the range from 0.1 g/L to 2 g/L. It is illustrated  
342 that phenol concentration decreases monotonically with an increase in catalyst mass in the water.  
343 It is obvious that the higher catalyst mass, the higher the area of the reactive surface available for  
344 adsorption and reaction will be. But the effect of catalysts dose cannot be indefinitely beneficial.  
345 Above a certain level, the degradation rate will remain constant even with increased catalysts  
346 loading. This rule is more obvious with  $\text{TiO}_2$  in Table (4). As the concentration of the catalyst  
347 increases, the amount of adsorbed photons as well as phenol molecules increases with respect to  
348 the number of catalysts molecules. The concentration in the area of illumination also increases



349 and thus the reaction rate is enhanced. All studies of photocatalysis note the existence of an  
 350 optimal concentration of TiO<sub>2</sub>. It can be concluded that a suitable amount of TiO<sub>2</sub> for the  
 351 photocatalytic reaction is approximately 1-3 g/L depending on types of reactor and TiO<sub>2</sub> powders  
 352 [19, 21]. In our experiment, the catalyst loading is approximately 1.5 g/L for undoped TiO<sub>2</sub>,  
 353 while it can be in excess of 2 g/L for Cu doped TiO<sub>2</sub>. Previous researchers suggest [24] that  
 354 high-TiO<sub>2</sub> dose might lead to aggregation of the catalyst particles accompanied by reduction in  
 355 reactive sites. Furthermore, shielding effects may occur due to high turbidity along with high  
 356 concentration of catalyst which prevents light penetration. A consequent rate decrease is always  
 357 a possibility if the dose is increased above a certain limit and hence the catalyst concentration  
 358 must be monitored to ensure efficient photodegradation.

### 359 3.4 The effect of solution pH

360 Industrial effluents may be basic or acidic and therefore the effect of pH should be investigated.  
 361 The pH value of phenol solution has a significant influence on the photocatalytic process for a  
 362 variety of reasons, including the TiO<sub>2</sub> surface charge state, the flat-band potential, and the  
 363 dissociation of phenol. These processes all are strongly pH dependent. The relative  
 364 concentration of functional groups on the surface of hydrated TiO<sub>2</sub> (TiOH<sub>2</sub><sup>+</sup>, TiOH and TiO<sup>-</sup>)  
 365 varies depending on the pH, due to surface hydroxyl groups gaining or losing a proton.



370 For Degussa P25 TiO<sub>2</sub>, pKa<sub>1</sub>= 4.5 and pKa<sub>2</sub> = 8. The pH of the point of zero charge, pH<sub>pzc</sub>, can  
 371 be calculated from half of the sum of pKa<sub>1</sub> and pKa<sub>2</sub>: pH<sub>pzc</sub> = 6.25. The surface of TiO<sub>2</sub> shows a  
 372 net positive charge as pH decrease below the pH<sub>pzc</sub> and the negative charged surface dominates

373 as pH increases above  $\text{pH}_{\text{pzc}}$ . Phenol ( $\text{p}K_{\text{a}}= 9.95$ ) exists as a molecular form in a neutral and  
374 weakly basic solutions. High pH value favours the dissociation of phenol into phenoxide ion  
375  $\text{C}_6\text{H}_5\text{O}^-$ . As illustrated in Figure (5), a decrease in pH decreases the degradation rate. There is  
376 less discrepancy between the neutral and basic environment, as compared to acidic conditions,  
377 which may be explained by the surface chemistry of the system. At a low pH = 3.3 the molecule  
378 of phenol is non-dissociated (neutral) and the surface of  $\text{TiO}_2$  is either at a neutral state ( $\text{TiOH}$ )  
379 [24] or positively charged as suggested by Al-Ekabi et al. [25]. These researchers studied the  
380 photocatalytic oxidation of chlorinated phenol solutions and observed that the protonation of the  
381  $\text{TiO}_2$  surface at low pH might be responsible for the inhibition of  $\text{TiO}_2$ -mediated adsorption of  
382 chlorinated hydrocarbon. In this study, as the pH is adjusted with HCl, the  $\text{Cl}^-$  anions are also  
383 adsorbed at the surface of  $\text{TiO}_2$ . There is competition between the adsorption of the anions and  
384 phenol, hence the generation of  $\text{OH}\cdot$  radicals is retarded. In the case of substances which are  
385 weakly acidic, the photocatalytic degradation of phenol increases at lower pH because of an  
386 increase in adsorption. At  $\text{pH}= 6.3$ , which is near its theoretical isoelectric point, the surface of  
387  $\text{TiO}_2$  is negatively charged while the phenol adsorption is at its maximum and the quantity of  $\text{Cl}^-$   
388 ions is lower [24]. Meanwhile, when the pH increases, the active hydroxyl groups on the  $\text{TiO}_2$   
389 surface increase accordingly. Consequently, a faster generation of  $\text{OH}\cdot$  radicals accelerates the  
390 phenol oxidation [21]. It is also consistent with the work of O'Shea and Cardona [26], who found  
391 that the initial reaction rates for phenol degradation steadily increases in the pH range from 3.0 to  
392 9.0, however a lack of significant acceleration in the initial reaction rates was found at higher  
393 pH. Similarly in our experiment, there is no significant difference in the initial reaction rate at a  
394 pH of 10.3. This can be attributed to the fact that phenol is entirely dissociated into phenoxide  
395 ion, which will compete for the reactive sites with the  $-\text{OH}$  groups and reduce the  $\text{OH}\cdot$  radicals.

396 Meanwhile, there is a phenomenon of repulsion between the negatively charged surface of  $\text{TiO}_2$   
397 and phenoxide ions, which explains the decrease in the rate of phenol oxidation. Although the  
398 pH dependence phenomena have been observed by many authors, detailed explanations are still  
399 not conclusive. Okamoto et al. [27] studied the photocatalytic oxidation of a 1 mM phenol  
400 solution with  $\text{TiO}_2$  and suggested that the optimum pH value was 3.5. Augugliaro et al. [19]  
401 found that the kinetic rate increased as the pH value increased to about 3, and then it decreased  
402 steadily until a pH value of about 12.5, beyond which the reaction rate constant again sharply  
403 increased. Some other investigators have reported no effect of pH on the rate of phenol removal.

#### 404 *3.5 The effect of light intensity*

405 Since the  $\text{TiO}_2$  powder is suspended in a stirred solution, the light intensity will affect the degree  
406 of light absorption by the  $\text{TiO}_2$  surface [21]. Previous investigators have also studied the light-  
407 intensity effect on the phenol degradation [27]. There are two ways of varying the light source  
408 intensity in our solar box system. One is to change the distance of light and batch reactor.  
409 Another is simply changing the light input sources, comparing UVA light with natural sunlight.

410

##### 411 *3.5.1 Comparison between dark and irradiation*

412 In our batch reactor system, the catalyst used in this experiment is  $\text{TiO}_2$  P25. Control is achieved  
413 by exposing phenol in the solar box system, while another flask containing phenol and the same  
414 amount of  $\text{TiO}_2$  is kept in the dark during the same experiment period.

415 It is evident in Figure (6) that the presence of both catalyst and irradiation act favourably in the  
416 photocatalytic process. In the absence of  $\text{TiO}_2$  P25, phenol can hardly be degraded during a time  
417 period over 20 h. Similar trends can be observed for the absence of irradiation, which also  
418 suggests that  $\text{TiO}_2$  powder cannot promote the oxidation of phenol [21] and that the adsorption

419 of phenol is negligible in the dark. The decline of phenol in the presence of  $\text{TiO}_2$  along with  
420 UVA irradiation may be attributed to the photooxidation process rather than adsorption.

421

### 422 *3.5.2 Comparison between the position of flask container*

423 In our batch reactor system, 100 mL quartz flasks are employed as the container which can be  
424 placed either in position “A” that is just next to the lamp assuming the distance to be 0 cm or  
425 position “B” that has a distance of 10 cm from the lamp. It is clear from Figure (7) that the nearer  
426 the flask is to the lamp, the more efficient the photodegradation of phenol in the solar box. The  
427 obvious explanation is that in the position “A”, the same size flask received more irradiation than  
428 the flask in position “B”. Hence, it suggests that in the design of reactor system, effort can be  
429 made to reduce the space between the reactor and the lamp.

430

### 431 *3.5.3 Comparison between artificial UVA and sunlight*

432 The threshold wavelength corresponds to the band gap energy for the semiconductor catalyst,  
433 e.g., for the  $\text{TiO}_2$  catalyst having band gap energy of 3.02 eV, the ideal wavelength is 400 nm.  
434 Sunlight therefore is a valid source of irradiation for the excitation of the catalyst and has a  
435 considerable economic advantage. A direct comparison between the results with solar box  
436 system and sunlight from a clear sky is shown in Figure (8). The control shows no sign of phenol  
437 degradation under sunlight. In the presence of  $\text{TiO}_2$ , the concentration of phenol drops to around  
438 10 mg/l in 5 hours, indicating 80% degradation. By comparing the sunlight and the solar box, it  
439 can be seen that the former is almost 4 times more efficient than the latter. Similarly, it has been  
440 reported [28] that the time required for 90% degradation of the phenol in sunlight in the presence  
441 of 0.1%  $\text{TiO}_2$  suspension was 55 min, approximately 1.7 times less than with the 100 W medium

442 pressure mercury lamp. The results confirmed the possibility of substitute UV irradiation with  
443 direct sunlight. At the same time, data obtained in the solar box system can be extrapolated from  
444 the laboratory set-up to a larger scale with reasonable confidence.

### 445 *3.6 The effect of catalysts preparation method*

446 The properties of catalysts are very much dependant on the preparation methods, therefore, two  
447 different preparation methods for doped TiO<sub>2</sub> were used as specified in Table (5). As depicted in  
448 Figure (9), IMTCu2 exhibits a better efficiency than SGTCu17 in phenol degradation, both of  
449 which are prepared from CuCl<sub>2</sub> at a same concentration. The different in preparation methods  
450 determine the dopant concentration distribution in the TiO<sub>2</sub> lattice structure, which may explain  
451 the variation in photoactivity. In the wet impregnation method, the dopants may be confined to  
452 the surface and/or to a few top layers of TiO<sub>2</sub> particles as dispersed species due to the moderate  
453 calcination temperatures. The dopants in the sol gel methods are homogenously “dissolved” in  
454 the TiO<sub>2</sub>, although further calcinations may change their concentration distribution, the sol gel  
455 method may produce a more homogenous doped catalyst, which is not always favoured.

456

457  
458  
459  
460  
461  
462  
463  
464  
465  
466

467 **Conclusions:**

468 In the solar box system with two 18W UVA lamps, undoped TiO<sub>2</sub> and Cu doped TiO<sub>2</sub> showed  
469 considerable phenol degradation. The efficiency of photocatalytic reaction largely depends on  
470 the photocatalysts and the methods of preparation the photocatalysts. The doping of Fe, Mn, and  
471 humic acid at 1.0 M% via sol gel methods were detrimental for phenol degradation. The  
472 unremarkable inhibitory effect of initial phenol concentration on initial phenol degradation rate  
473 reveals that photocatalytic decomposition of phenol follows pseudo zero order reaction kinetics.  
474 A concentration of at least 1 g/L TiO<sub>2</sub> and Cu doped TiO<sub>2</sub> is required for the effective  
475 degradation of 50 mg/L of phenol at neutral pH. It was found that pH plays a major role in the  
476 phenomena of adsorption of phenol onto TiO<sub>2</sub>. The increase in OH<sup>-</sup> concentrations at a higher pH  
477 values is beneficial of phenol degradation. However, the competition between phenoxide ion, Cl<sup>-</sup>  
478 and OH<sup>-</sup> for the limited number of reactive sites on TiO<sub>2</sub> will be a negative factor in the  
479 generation of hydroxyl radical. TiO<sub>2</sub> is not active in the dark and the adsorption is negligible. The  
480 dependence of phenol degradation rate on the light intensity was investigated, with the results  
481 implying that direct sunlight can be a substitute for UV lamps, and that photocatalytic treatment  
482 of organic pollutants may be an efficient technique.

483

484

485

486

487

488

489

490 **References:**

- 491 [1] L.M. Fry, J.R. Mihelcic, D.W. Watkins, Water and nonwater-related challenges of achieving  
492 global sanitation coverage, *Environ. Sci. Technol.* 42 (2008) 4298–4304.  
493
- 494 [2] E.H. Goslan, S.W. Krasner, M. Bower, S.A. Rocks, P. Holmes, L.S. Levy, S.A. Parsons, A  
495 comparison of disinfection by-products found in chlorinated and chloraminated drinking waters  
496 in Scotland, *Water Res.* 43 (2009) 4698–4706.  
497
- 498 [3] S. Valencia, F. Cataño, L. Rios, G. Restrepo, J. Marín, A new kinetic model for  
499 heterogeneous photocatalysis with titanium dioxide: Case of non-specific adsorption considering  
500 back reaction. *App. Cata. B: Env.* 104 (2011) 300–304.  
501
- 502 [4] H. Sun, S. Wang, H. Ang, M.O. Tadé, Q. Li. Halogen element modified titanium dioxide for  
503 visible light photocatalysis. *Chem. Eng. J.* 162 (2010) 437–447.  
504
- 505 [5] D. Ravelli, D. Dondib, M. Fagnonia, A. Albinia, Titanium dioxide photocatalysis: An  
506 assessment of the environmental compatibility for the case of the functionalization of  
507 heterocyclics. *App. Cata. B: Env.* 99 (2010) 442–447.  
508
- 509 [6] G. Hyett, M.A. Greenb, I.P. Parkina, Ultra-violet light activated photocatalysis in thin films  
510 of the titanium oxynitride,  $Ti_{3-x}O_{4-x}N_x$ . *J. Photochem. Photobiol. A: Chem.* 203 (2009) 199–203.  
511
- 512 [7] T. Matsunaga, R. Tomoda, T. Nakajima, H. Wake, Photoelectrochemical sterilization of  
513 microbial-cells by semiconductor powders. *Fems Micro. Lett.* 29 (1985) 211-214.
- 514 [8] J.C. Ireland, E. Klostermann, W. Rice, R.M. Clark, Inactivation of *Escherichia coli* by  
515 titanium dioxide photocatalytic oxidation. *Appl. Environ. Microbiol.* 59 (1993) 1668-1670.
- 516 [9] Y. Ide, M. Matsuoka, M. Ogawa, Efficient visible-light-induced photocatalytic activity on  
517 gold-nanoparticle-supported layered titanate. *J. Am. Chem. Soc.* 132 (2010) 16762–16764.  
518
- 519 [10] G. Zhang, X. Ding, Y. Hu, B. Huang, X. Zhang, X. Qin, J. Zhou, J. Xie, Photocatalytic  
520 degradation of 4BS dye by N,S-codoped  $TiO_2$  pillared montmorillonite photocatalysts under  
521 visible-light irradiation. *J. Phys. Chem. C.* 112 (2008) 17994–17997.  
522
- 523 [11] Y. Li, J. Wang, B. Liu, L. Dang, H. Yao, Z. Li, BiOI-sensitized  $TiO_2$  in phenol degradation:  
524 A novel efficient semiconductor sensitizer. *Chem. Phy. Lett.* 508 (2011) 102–106.  
525
- 526 [12] L. Zhu, C. He, Y. Huang, Z. Chen, D. Xia, M. Su, Y. Xiong, S. Li, D. Shu, Enhanced  
527 photocatalytic disinfection of *E. coli* 8099 using Ag/BiOI composite under visible light  
528 irradiation. *Sep. Purif. Tech.* 91 (2012) 59–66.  
529
- 530 [13] M. Liga, E. Bryan, V. Colvin, Q. Li, Virus inactivation by silver doped titanium dioxide  
531 nanoparticles for drinking water treatment. *Water Res.* 45 (2011) 535-544.  
532

- 533 [14] S. Sontakke, C. Mohan, J. Modak, G. Madras, Visible light photocatalytic inactivation of  
534 *Escherichia coli* with combustion synthesized TiO<sub>2</sub>. *Chem. Eng. J.* 189–190 (2012) 101– 107.  
535
- 536 [15] X.Z. Ding, X.H. Liu, Synthesis and microstructure control of nanocrystalline titania  
537 powders via a sol-gel process. *Mat. Sci. Eng. A-Struct. Mat Prop Microst Proc.* 224 (1997) 210-  
538 215.
- 539 [16] A. Di Paola, E. Garcia-Lopez, S. Ikeda, G. Marci, B. Ohtani, L. Palmisano, Photocatalytic  
540 degradation of organic compounds in aqueous systems by transition metal doped polycrystalline  
541 TiO<sub>2</sub>. *Cata Today.* 75 (2002) 87-93.
- 542 [17] J.C. Colmenares, M.A. Aramendia, A. Marinas, J.M. Marinas, F.J. Urbano, Synthesis,  
543 characterization and photocatalytic activity of different metal-doped titania systems. *App. Cata.*  
544 *A-General.* 306 (2006) 120-127.
- 545 [18] V. Brezova, A. Blazkova, L. Karpinsky, J. Groskova, B. Havlinova, V. Jorik, M. Ceppan,  
546 Phenol decomposition using Mn<sup>+</sup>/TiO<sub>2</sub> photocatalysts supported by the sol-gel technique on  
547 glass fibres. *J. Photochem Photobio A-Chem.* 109 (1997) 177-183.
- 548 [19] V. Augugliaro, L. Palmisano, A. Sclafani, C. Minero, E. Pelizzetti, Photocatalytic  
549 Degradation of Phenol in Aqueous Titanium-Dioxide Dispersions. *Toxicolog. Env. Chem.* 16  
550 (1988) 89-109.
- 551 [20] K. Okamoto, Y. Yamamoto, H. Tanaka, M. Tanaka, A. Itaya, Heterogeneous Photocatalytic  
552 Decomposition of Phenol over TiO<sub>2</sub> Powder. *Bull. Chem. Soc. Japan.* 58 (1985) 2015-2022.
- 553 [21] T.Y. Wei, C.C. Wan, Heterogeneous Photocatalytic Oxidation of Phenol with Titanium-  
554 Dioxide Powders. *Ind. Eng. Chem. Res.* 30 (1991) 1293-1300.
- 555 [22] M. Primet, P. Pichat, M.V. Mathieu, Infrared Study of Surface of Titanium Dioxides .2.  
556 Acidic and Basic Properties. *J. Phy. Chem.* 75 (1971) 1221-1225.
- 557 [23] S. Malato, P. Fernandez-Ibanez, M.I. Maldonado, J. Blanco, W. Gernjak, Decontamination  
558 and disinfection of water by solar photocatalysis: Recent overview and trends. *Cata. Today.* 147  
559 (2009) 1-59.
- 560 [24] S. Bakkouche, M. Bouhelassa, N.H. Salah, F.Z. Meghlaoui, Study of adsorption of phenol  
561 on titanium oxide (TiO<sub>2</sub>). *Desalin.* 166 (2004) 355-362.
- 562 [25] H. Alekabi, N. Serpone, E. Pelizzetti, C. Minero, M. A. Fox, R.B. Draper, Kinetic-Studies  
563 in Heterogeneous Photocatalysis .2. Tio<sub>2</sub>-Mediated Degradation of 4-Chlorophenol Alone and in  
564 A 3-Component Mixture of 4-Chlorophenol, 2,4-Dichlorophenol, and 2,4,5-Trichlorophenol in  
565 Air-Equilibrated Aqueous-Media. *Langm.* 5 (1989) 250-255.
- 566 [26] K.E. Oshea, C. Cardona, The Reactivity of Phenol in Irradiated Aqueous Suspensions of  
567 TiO<sub>2</sub> - Mechanistic Changes As A Function of Solution pH. *J. Photochem. Photobiol. A-Chem.*  
568 91 (1995) 67-72.



- 569 [27] K. Okamoto, Y. Yamamoto, H. Tanaka, A. Itaya, Kinetics of Heterogeneous Photocatalytic  
570 Decomposition of Phenol Over Anatase TiO<sub>2</sub> Powder. Bull. Chem. Soc. Japan. 58 (1985) 2023-  
571 2028.
- 572 [28] R.W. Matthews, S.R. Mcevoy, Photocatalytic Degradation of Phenol in the Presence of  
573 Near-UV illuminated Titanium-Dioxide. J. Photochem. Photobiol. A-Chem. 64 (1992) 231-246.

ACCEPTED MANUSCRIPT

574

Name	Chemical Formula	Manufacturer	Description
<b>Sol-gel method</b>			
Titanium (IV) isopropoxide(TTIP)	Ti(OC <sub>4</sub> H <sub>9</sub> ) <sub>4</sub>	Acros Organic, UK	metal alkoxides precursor
Anhydrous isopropanol	(CH <sub>3</sub> ) <sub>2</sub> CHOH	Acros Organic, UK	alcohol solvent
Anhydrous 2(2-ethoxyethoxy) ethanol	CH <sub>3</sub> CH <sub>2</sub> OCH <sub>2</sub> CH <sub>2</sub> O-CH <sub>2</sub> CH <sub>2</sub> OH	Acros Organic, UK	alcohol solvent
Anhydrous ethanol	CH <sub>3</sub> CH <sub>2</sub> OH	BDH chemicals, UK	alcohol solvent
37% Hydrochloric Acid	HCl	Fisher Chemicals, UK	hydrolysis catalyst
Sulphuric acid	H <sub>2</sub> SO <sub>4</sub>	BDH chemicals, UK	hydrolysis catalyst
Anhydrous copper (II) chloride	CuCl <sub>2</sub>	Acros Organic, UK	dopant
Anhydrous cupric sulphate	CuSO <sub>4</sub>	BDH chemicals, UK	dopant
Anhydrous copper (II) nitrate	Cu(NO <sub>3</sub> ) <sub>2</sub>	Fisher Chemicals, UK	dopant
Anhydrous Manganese chloride	MnCl <sub>2</sub>	Fisher Chemicals, UK	dopant
Iron(II) chloride	FeCl <sub>3</sub>	Fisher Chemicals, UK	dopant
Humic acid	n/a	Acros Organic, UK	dopant
<b>Wet-impregnation method</b>			
Anhydrous copper (II) chloride	CuCl <sub>2</sub>	Acros Organic, UK	dopant
Anhydrous cupric sulphate	CuSO <sub>4</sub>	BDH chemicals, UK	dopant
Titania P25	TiO <sub>2</sub>	DegussaCo. Germany	80% anatase, 20% rutile; BET area: 50 m <sup>2</sup> g <sup>-1</sup>

**Table 1:** Materials used in sol-gel method.

575  
576  
577  
578  
579  
580

581  
582  
583  
584  
585  
586  
587  
588  
589  
590

**Table 2:** Summary of photocatalysts used in preliminary experiment.

<b>Material</b>	<b>Sample</b>	<b>Treatment</b>
Cu doped TiO <sub>2</sub> from sol gel method	SGTCu17	Hydrolysis and condensation of sol mixture (TTIP: Ethanol: HCl: H <sub>2</sub> O: CuCl <sub>2</sub> = 1:8:0.3:1: 0.01) at room temperature and followed by drying at 500 °C for 2 h
Mn Doped TiO <sub>2</sub> from sol gel method	SGTMn1	Hydrolysis and condensation of sol mixture (TTIP: Ethanol: HCl: H <sub>2</sub> O:MnCl <sub>2</sub> =1:8:0.3: 1:0.01) at room temperature and followed by drying at 500 °C for 2 h
Iron doped TiO <sub>2</sub> from sol gel method	SGTFe1	Hydrolysis and condensation of sol mixture (TTIP: Ethanol: HCl: H <sub>2</sub> O:FeCl <sub>3</sub> =1:8:0.3: 1:0.01) at room temperature and followed by drying at 500 °C for 2 h
Humic acid doped TiO <sub>2</sub> from sol gel method	SGTHA1	Hydrolysis and condensation of sol mixture (TTIP: Ethanol: HCl: H <sub>2</sub> O: humic acid=1:8:0.3:1:0.01) at room temperature and followed by drying at 120 °C for 2 h
Undoped TiO <sub>2</sub> from sol gel method	SGT5	Hydrolysis and condensation of sol mixture (TTIP: Ethanol: HCl: H <sub>2</sub> O=1:8:0.3:1) at room temperature and followed by drying at 500 °C for 2 h

591  
592  
593  
594  
595  
596  
597  
598  
599  
600  
601  
602  
603

604  
605  
606  
607  
608  
609  
610  
611  
612  
613  
614  
615

**Table 3:** The initial phenol concentration effect on phenol disappearance rate on TiO<sub>2</sub> (Sample SGT5) and Cu doped TiO<sub>2</sub> (Sample SGTCu17) suspension from different initial concentration: 10 mg/L, 20 mg/L, 50 mg/L and 100 mg/L. Container size= 100 mL, Catalyst dose = 1g/L, pH = 6.3, Temp = 25°C.

phenol 1/[C <sub>0</sub> ], (L mol <sup>-1</sup> )	TiO <sub>2</sub> (1/r <sub>0</sub> ) (L min mmol <sup>-1</sup> )	Cu- TiO <sub>2</sub> (1/r <sub>0</sub> ) (L min mmol <sup>-1</sup> )
940	-1.681 × 10 <sup>4</sup>	-5.908 × 10 <sup>3</sup>
1880	-1.573 × 10 <sup>4</sup>	-5.048 × 10 <sup>3</sup>
4700	-1.147 × 10 <sup>4</sup>	-3.518 × 10 <sup>3</sup>
9400	-6.123 × 10 <sup>3</sup>	-2.874 × 10 <sup>3</sup>

616  
617  
618  
619  
620  
621  
622  
623  
624  
625  
626  
627  
628  
629  
630  
631  
632  
633  
634  
635  
636  
637  
638  
639  
640

641  
642  
643  
644  
645  
646  
647  
648  
649  
650  
651  
652

**Table 4:** Rate constants and binding constants from Langmuir-Hinshelwood plots for phenol disappearance on TiO<sub>2</sub> (Sample SGT5) and Cu doped TiO<sub>2</sub> (Sample SGTCu17) suspension from different initial concentration: 10 mg/L, 20 mg/L, 50 mg/L and 100 mg/L. Container size = 100 mL, Catalysts dose = 1g/L, pH = 6.3, Temp = 25°C.

Catalysts	Rate constant $k$ (mmol L <sup>-1</sup> min <sup>-1</sup> )	Binding constant $K$ (L mmol <sup>-1</sup> )
TiO <sub>2</sub>	$-0.16 \times 10^{-3}$	-17.57
Cu/TiO <sub>2</sub>	$-0.50 \times 10^{-4}$	-15.67

653  
654  
655  
656  
657  
658  
659  
660  
661  
662  
663  
664  
665  
666  
667  
668  
669  
670  
671  
672  
673  
674  
675  
676  
677  
678  
679  
680

681  
682  
683  
684  
685  
686  
687  
688  
689

**Table 5:** The catalyst dose effect on phenol disappearance rate on TiO<sub>2</sub> (Sample SGT5) and Cu doped TiO<sub>2</sub> (Sample SGTCu17) suspension in different catalysts dose: 0.1, 0.5, 1.0, 1.5 and 2.0 g/L. Container size = 100 mL, initial phenol concentration = 50 mg/L, pH = 6.3, Temp = 25°C.

Catalyst (g L <sup>-1</sup> )	TiO <sub>2</sub> r <sub>0</sub> (g h <sup>-1</sup> L <sup>-1</sup> )	Cu doped TiO <sub>2</sub> r <sub>0</sub> (g h <sup>-1</sup> L <sup>-1</sup> )
0.1	-0.00197	-4.94 × 10 <sup>-5</sup>
0.5	-0.00248	-4.15 × 10 <sup>-4</sup>
1.0	-0.00298	-8.95 × 10 <sup>-4</sup>
1.5	-0.00334	-9.85 × 10 <sup>-4</sup>
2.0	-0.00338	-11.8 × 10 <sup>-4</sup>

690  
691  
692  
693  
694  
695  
696  
697  
698  
699  
700  
701  
702  
703  
704  
705  
706  
707  
708  
709  
710  
711  
712  
713  
714  
715  
716  
717  
718  
719  
720  
721

722  
723  
724  
725  
726  
727

**Table 6:** Photocatalysts used in studying the effect of catalyst's preparation method.

<b>Material</b>	<b>Sample</b>	<b>Treatment</b>
Cu doped TiO <sub>2</sub> from sol-gel method	SGTCu17	Hydrolysis and condensation of sol mixture (TTIP: Ethanol: HCl: H <sub>2</sub> O: CuCl <sub>2</sub> = 1:8:0.3:1:0.01) at room temperature and followed by drying at 500 °C for 2 h
Cu doped TiO <sub>2</sub> from wet-impregnation method	IMTCu2	Magnetic stirring of aqueous mixture of CuCl <sub>2</sub> and TiO <sub>2</sub> P25 (molar ratio: 0.01) at room temperature for 24 h and followed by filtration, oven drying at 60 °C overnight and 500 °C for 2 h

728  
729  
730  
731

732 **Figure Captions:**

733

734 **Figure 1:** Schematic layout of continuous flow system.

735

736 **Figure 2:** Phenol disappearance on TiO<sub>2</sub> (Sample SGT8) and doped TiO<sub>2</sub> suspension. Container  
737 size = 25mL, Catalysts dose = 1g/L, initial phenol concentration = 50 mg/L, pH = 6.3, Temp =  
738 25°C.

739

740 **Figure 3:** Zero order plots of phenol disappearance on (a) TiO<sub>2</sub> (Sample SGT5) and (b) Cu  
741 doped TiO<sub>2</sub> (Sample SGTCu17) suspension from different initial concentration: 10mg/L,  
742 20mg/L, 50mg/L and 100mg/L. Container size = 100mL. Catalysts dose = 1g/L, pH = 6.3, T =  
743 25°C.

744

745 **Figure 4:** Phenol disappearance on (a) TiO<sub>2</sub> (Sample SGT5) and (b) Cu doped TiO<sub>2</sub> (Sample  
746 SGTCu17) suspension in different catalysts dose: 0.1, 0.5, 1.0, 1.5 and 2.0 g/L. Container size =  
747 100 mL, initial phenol concentration = 50 mg/L, pH = 6.3, T = 25°C.

748

749 **Figure 5:** Phenol disappearance from TiO<sub>2</sub> (Sample SGT5) suspension at different pH: 3.3, 6.3  
750 and 10.3. Catalysts dose = 1g/L, initial phenol concentration = 50 mg/L, container size = 100  
751 mL, T = 25°C.

752

753 **Figure 6:** Phenol disappearance on TiO<sub>2</sub> (Sample p25) suspension in different irradiation  
754 conditions: Dark and solar box system UVA irradiation. Container size = 100 mL, Catalysts dose  
755 = 1g/L, initial phenol concentration = 40 mg/L, pH = 6.3, T = 25°C. Control is used with absence  
756 of TiO<sub>2</sub> in solar box system.

757

758 **Figure 7:** Phenol disappearance on TiO<sub>2</sub> (Sample P25) suspension in at different distance from  
759 lamp: A is 0 cm and B is 10 cm. Container size = 100 mL, Catalysts dose = 1g/L, initial phenol  
760 concentration = 40 mg/L, pH = 6.3, T = 25°C.

761

762 **Figure 8:** Phenol disappearance on TiO<sub>2</sub> (Sample SGT5) suspension in different irradiation  
763 conditions: Direct sunlight and solar box system UVA irradiation. Container size = 100 mL,  
764 Catalysts dose = 1g/L, initial phenol concentration = 50 mg/L, pH = 6.3. Control is used with  
765 absence of TiO<sub>2</sub> in direct sunlight.

766

767 **Figure 9:** Phenol disappearance on Cu doped TiO<sub>2</sub> using sample prepared from different method  
768 sol gel (Sample SGTCu17) and wet-impreganation (Sample IMTCu2) in solar box system UVA.  
769 Container size = 100 mL, Catalysts dose = 1g/L, initial phenol concentration = 50 mg/L, pH =  
770 6.3. Control is used with absence of Cu-TiO<sub>2</sub> in the same solar box system.

771

772

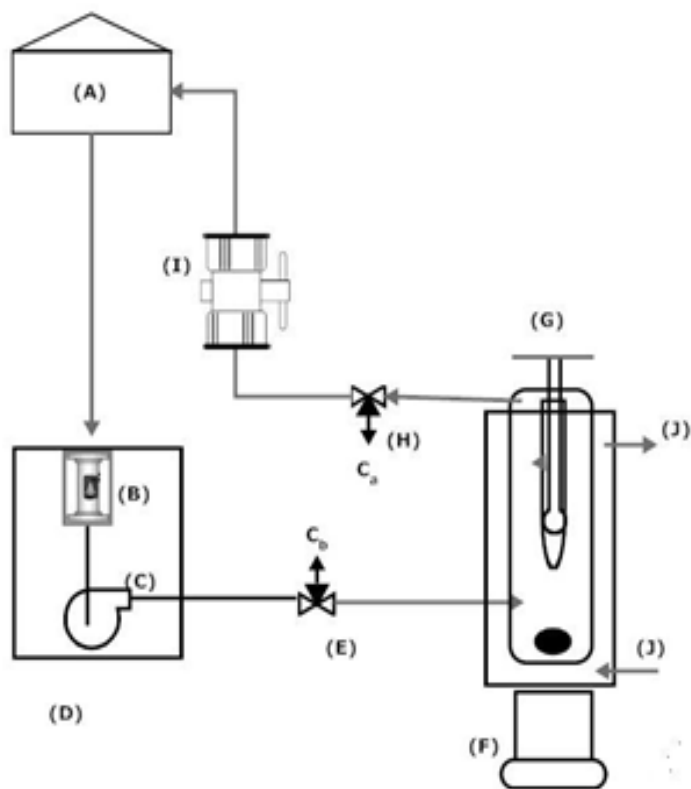
773

774

775

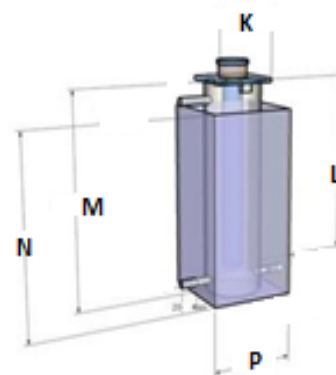


776 **Figure 1**  
777



**LIST OF COMPONENTS**

A - Tank	F - Magnetic Stirrer
B - Flow Meter	G - Lamp Reactor
C - DC Pump	H - Sampling Port $C_a$
D - Water Grab Sampler	I - Filter
E - Sampling Port $C_b$	J - Cooling tap water

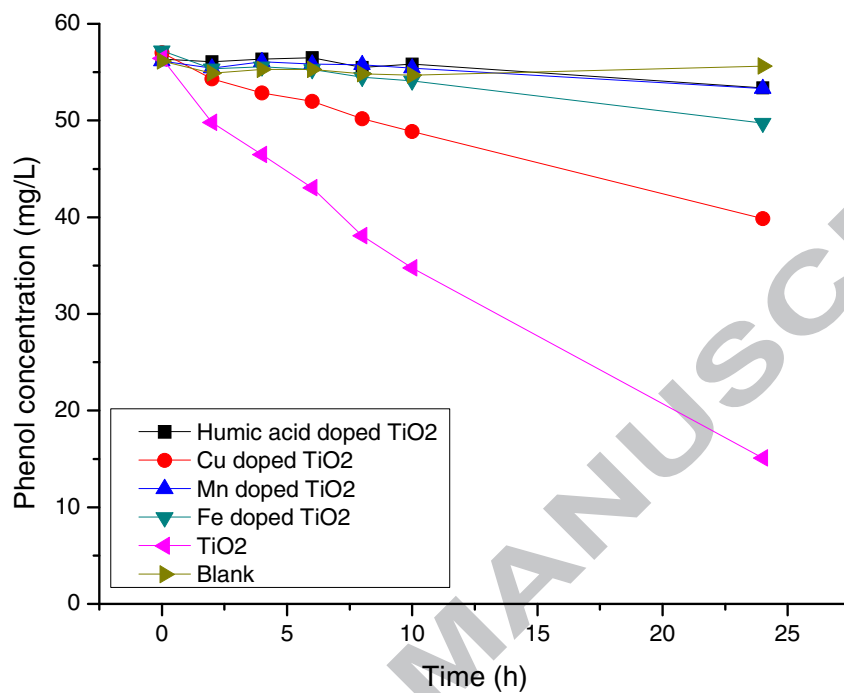


(G)

K= 71mm  
L= 220 mm  
M= 105mm  
N= 220mm  
P= 71mm

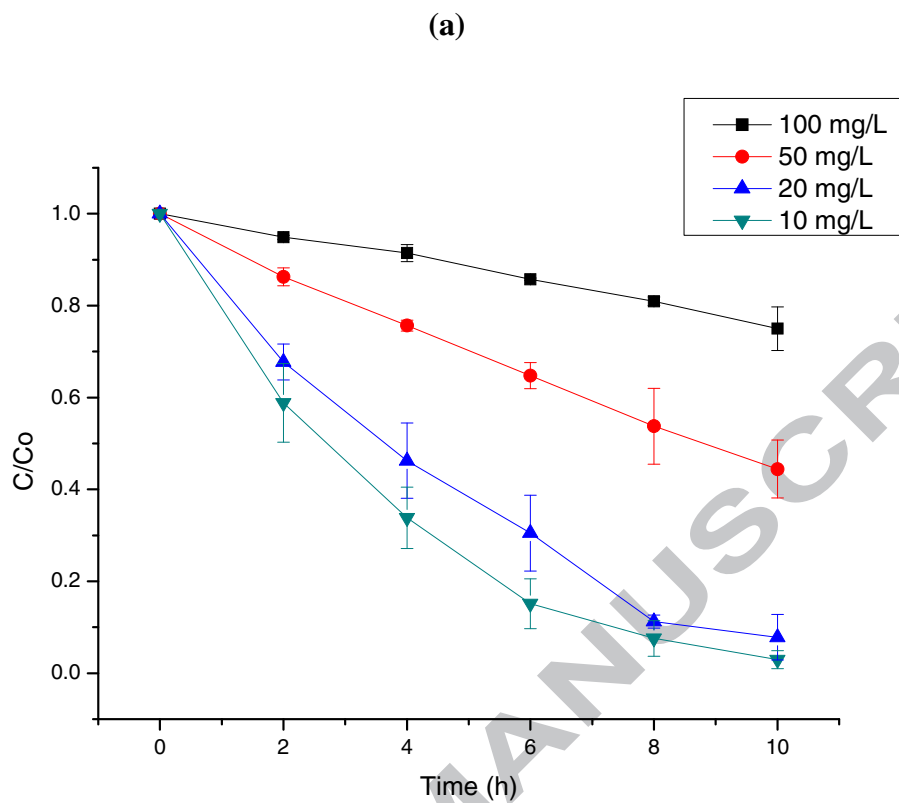
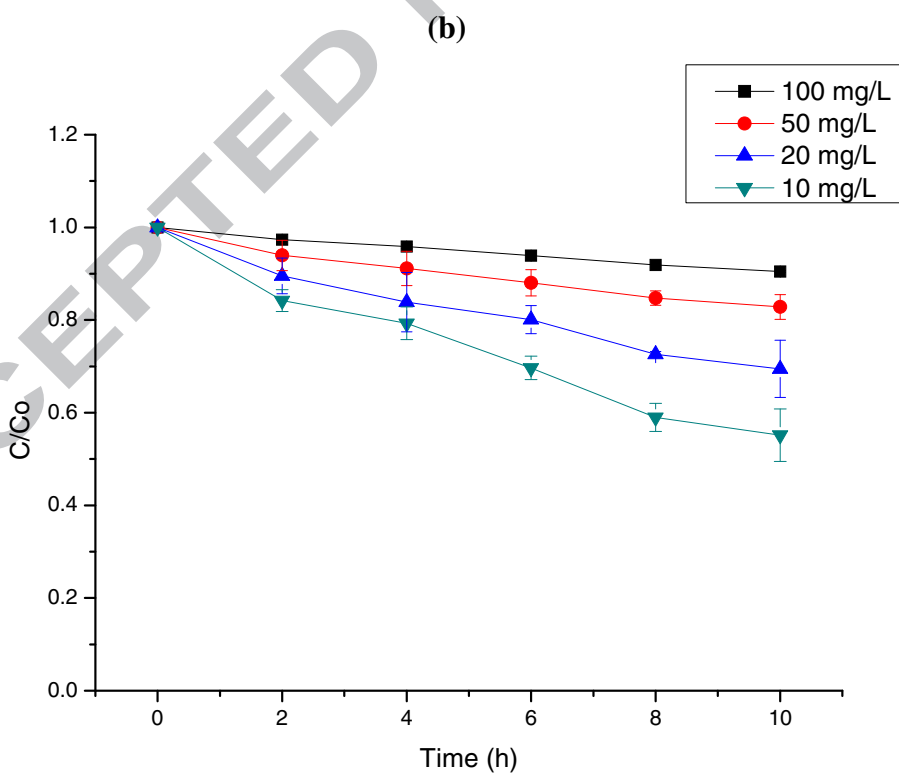
778  
779  
780  
781  
782  
783  
784  
785  
786  
787  
788  
789  
790  
791  
792  
793  
794  
795

796 **Figure 2**  
797



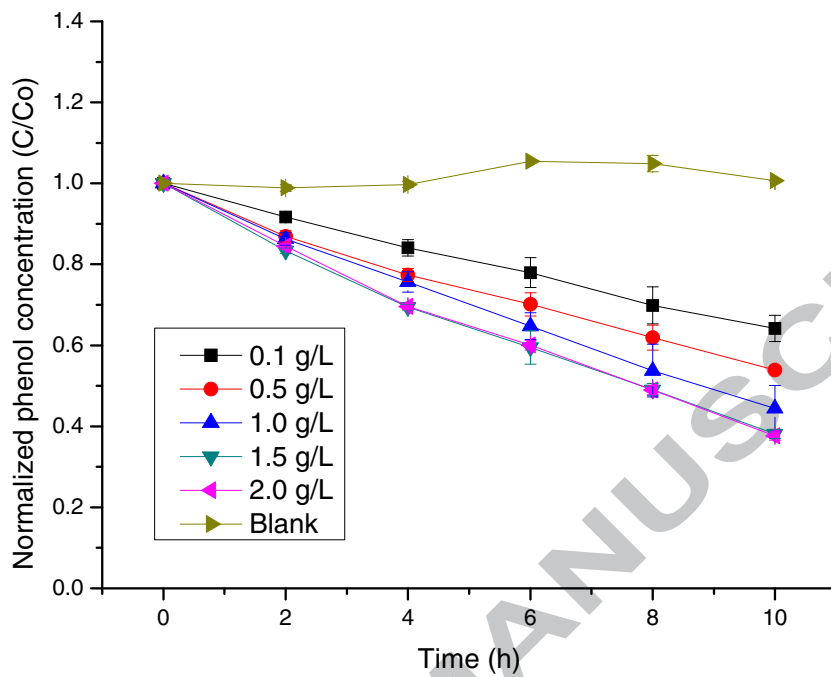
798  
799  
800  
801  
802  
803  
804  
805  
806  
807  
808  
809  
810  
811  
812  
813

**Figure 3**

814  
815816  
817818  
819 **Figure 4**

820

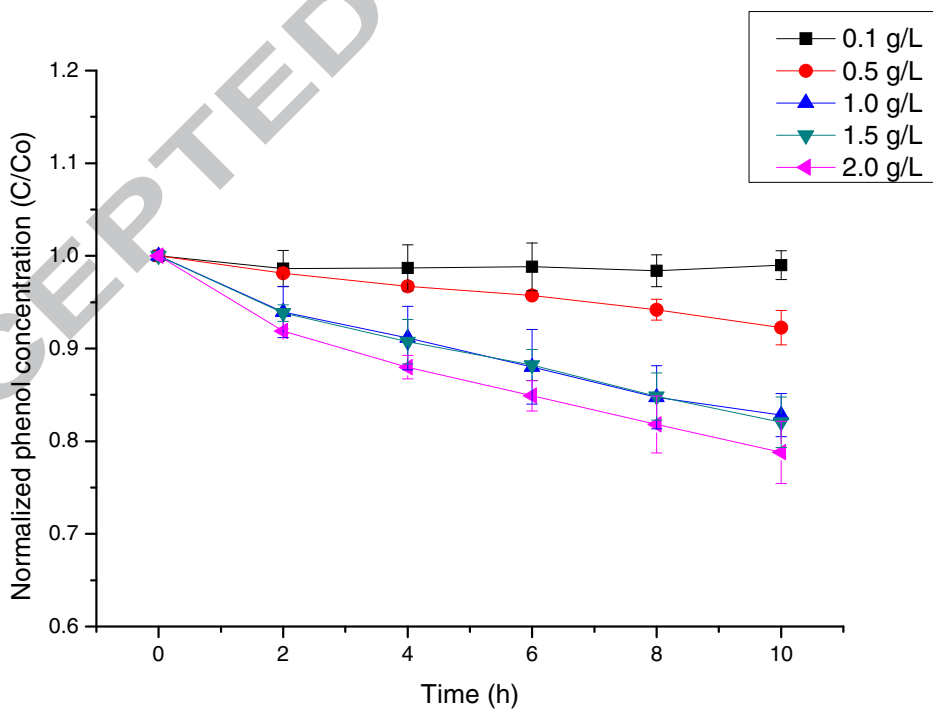
(a)



821

822

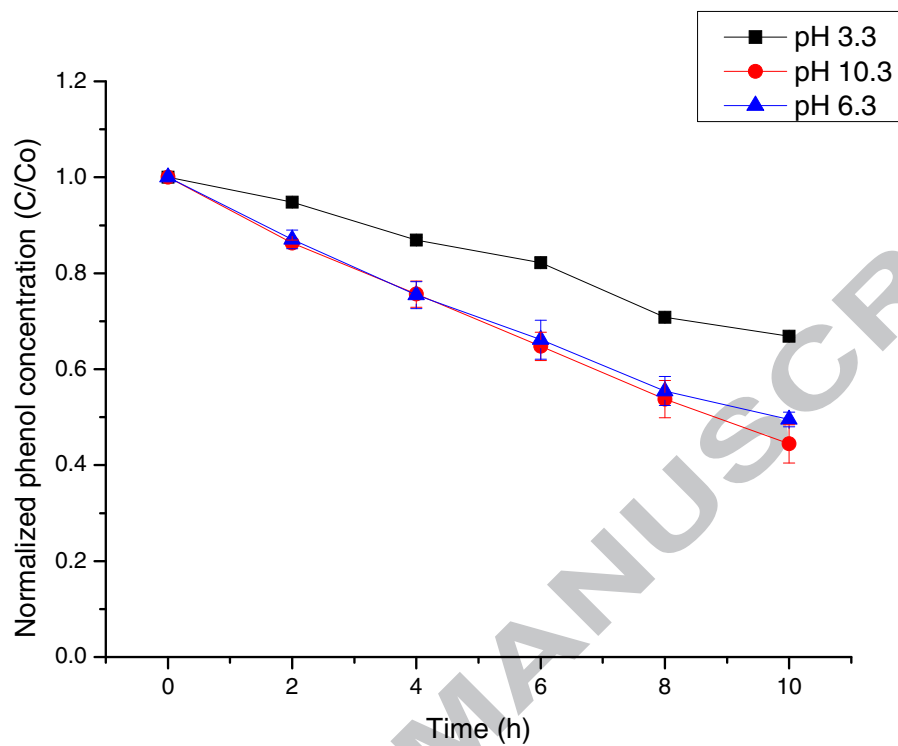
(b)



823

824 **Figure 5**

825



826

827

828

829

830

831

832

833

834

835

836

837

838

839

840

841

842

843

844

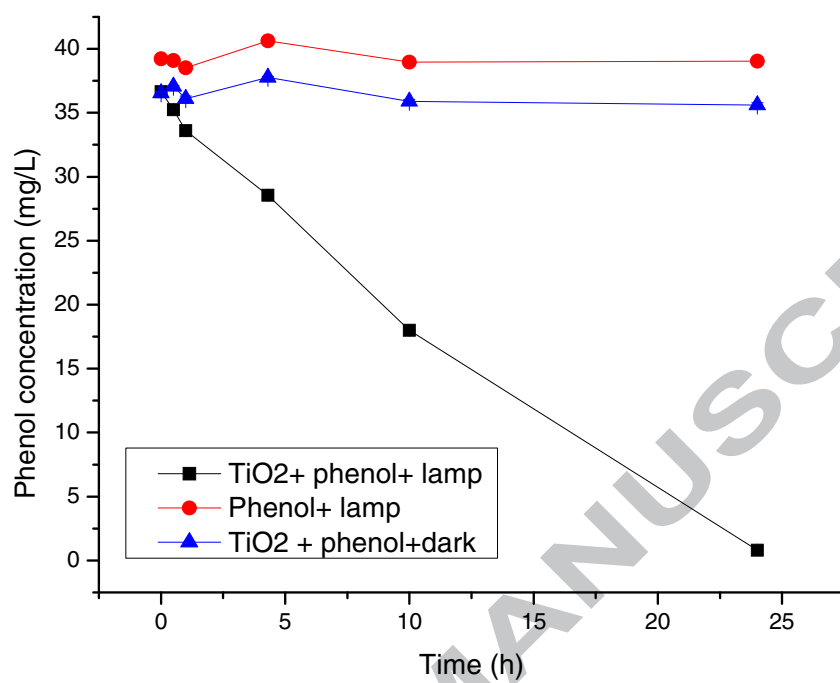
845

846

847

**Figure 6**

848



849

850

851

852

853

854

855

856

857

858

859

860

861

862

863

864

865

866

867

868

869

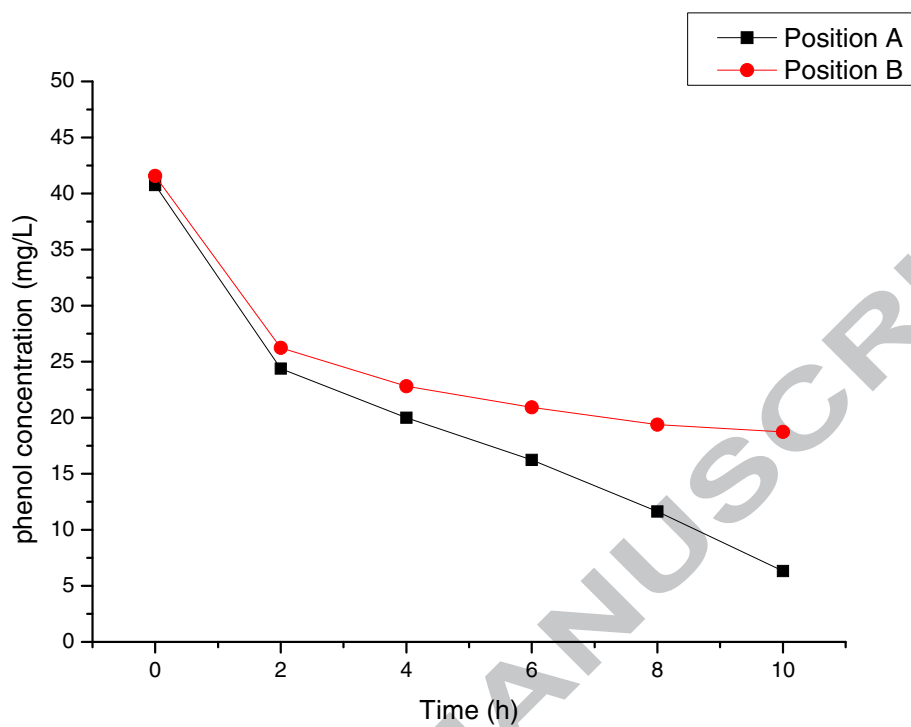
870

871

872

**Figure 7**

873



874

875

876

877

878

879

880

881

882

883

884

885

886

887

888

889

890

891

892

893

894

895

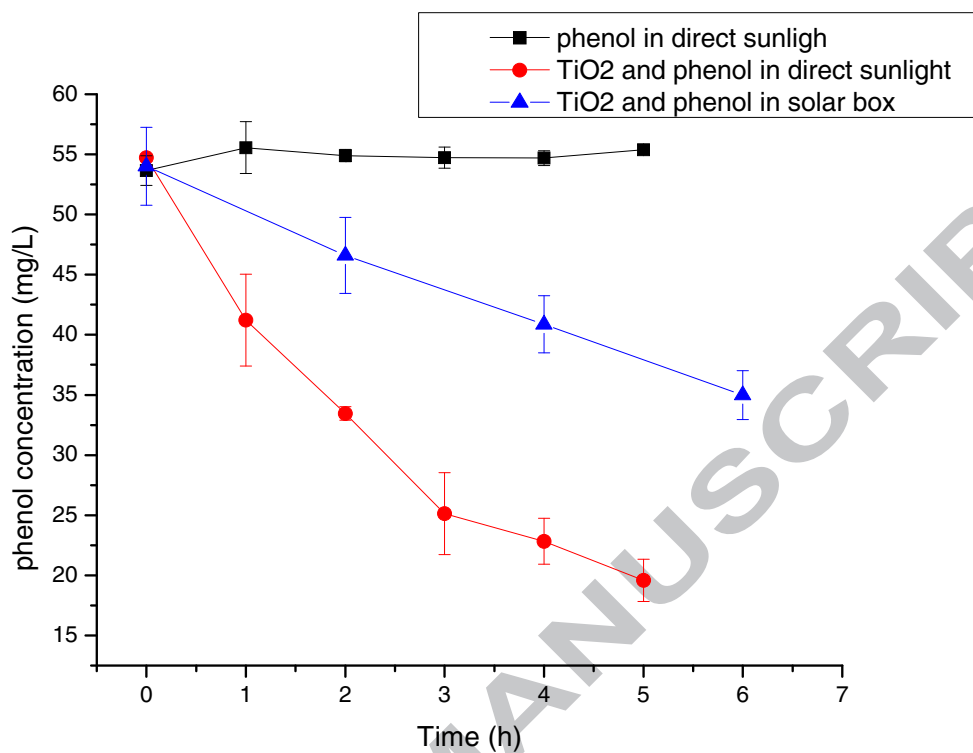
896

897

898

**Figure 8**

899



900

901

902

903

904

905

906

907

908

909

910

911

912

913

914

915

916

917

918

919

920

921

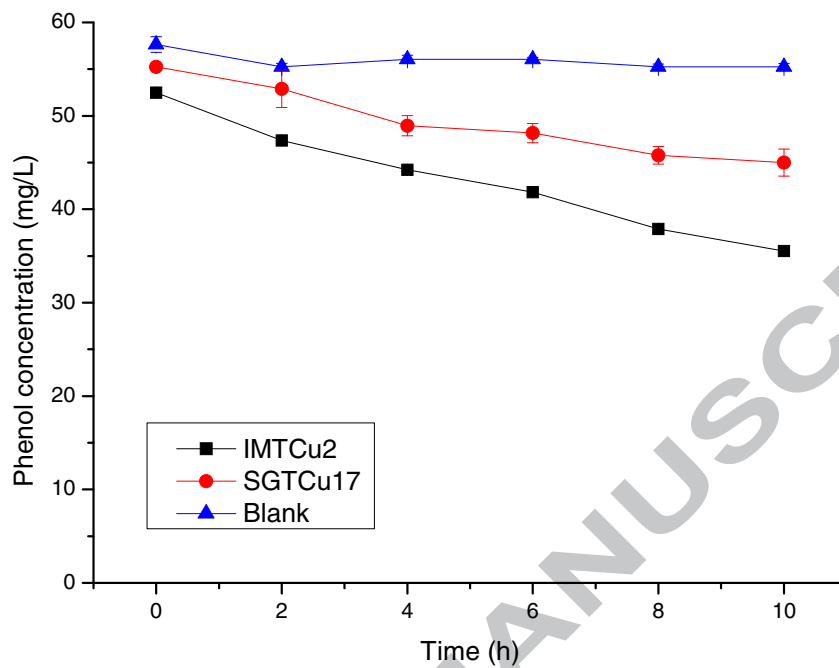
922

923

**Figure 9**



924



925

926

927

928

929

930

931

932

933

934

935

936

937

938

939 **Research Highlights:**

- 940 1- Removal of phenol by the application of TiO<sub>2</sub> based photocatalysts was explored.
- 941 2- Undoped TiO<sub>2</sub> and Cu doped TiO<sub>2</sub> showed considerable phenol degradation.
- 942 3- The efficiency of photocatalytic reaction depends on the methods of preparation.
- 943 4- Photocatalytic decomposition of phenol follows pseudo zero order reaction kinetics.
- 944 5- Direct sunlight can be a substitute for the UV lamps.

945

946

947

ACCEPTED MANUSCRIPT